CHARACTERISATION OF THE KURRI 150 MeV FFAG AND PLANS FOR HIGH INTENSITY EXPERIMENTS

S. L. Sheehy*, D. Kelliher, S. Machida, C. Rogers, C. R. Prior, ASTeC/STFC/RAL, United Kingdom
On behalf of the KURRI-FFAG collaboration

Abstract

Fixed field alternating gradient (FFAG) accelerators hold a lot of promise for high power operation due to their high repetition rate and strong focusing optics. However, to date these machines have not been operated with high intensity beams. Since November 2013 an experimental collaboration has been underway to characterise the 150 MeV proton FFAG at KURRI, Japan. Here we report on the results of characterisation experiments and discuss plans for further experiments in the high intensity regime.

INTRODUCTION

Fixed field Alternating Gradient (FFAG) accelerators combine strong focusing optics like a synchrotron with a fixed magnetic field like a cyclotron. Unlike a synchrotron, the magnetic field experienced by the particles is designed to vary with radius, rather than time. This naturally leads to the potential to operate at high repetition rates limited only by the available rf system, while strong focusing provides a possibility of maintaining higher intensity beams than in cyclotrons.

A revival in interest since the 1990s has seen a number of FFAGs constructed, including scaling and linear non-scaling variants. However, high bunch charge operation remains to be demonstrated. A collaboration has been formed to use an existing proton FFAG accelerator at Kyoto University Research Reactor Institute (KURRI) in Japan to explore the high intensity regime in FFAG accelerators. Work has so far been aimed at characterising this machine in detail. Later experiments will be aimed at demonstrating high bunch charge operation in an FFAG accelerator and exploring the fundamental intensity limitations of these machines.

The KURRI 150 MeV ADSR-FFAG

The 11–150 MeV ADSR-FFAG at KURRI [1] (shown in Fig. 1) is a scaling FFAG where the main magnetic field follows a power law with radius,

$$B_z(r) = B_0(r/r_0)^k. \tag{1}$$

The field index, k, is designed to be 7.6 and other parameters are given in Table 1.

The primary operational goal of the 150 MeV FFAG is to undertake basic studies toward the realisation of Accelerator Driven Systems (ADS) [2]. It is also used for irradiation experiments for industrial use, medical applications such as BNCT as well as radiobiology experiments.

* suzie.sheehy@stfc.ac.uk

Figure 1: The KURRI 150 MeV FFAG is the larger ring shown here with the pre-2011 injector ring. Injection from the new linac occurs in the top left of the image.

The ring consists of twelve DFD magnet triplets which are an innovative 'yoke-free' design [3] which allows the beam to be injected and extracted through the side of the magnets.

Originally injected by a low energy proton booster ring, in 2011 the injector was upgraded to an 11 MeV H$^-$ linac to increase the beam intensity from roughly 6×10^8 ppp to up to 3.12×10^{12} ppp [4]. The beam is now injected using H$^-$ charge exchange injection on a 20 μg.cm^{-2} carbon foil. No bump system is used as the beam moves radially away from the foil as it is accelerated.

At present the linac provides 10 nA average current (3.12×10^9 ppp) with a bunch length of 100 μs at injection and 0.1 μs at extraction, operating at a 20 Hz repetition rate. In principle the linac can provide up to 5 μA average current.

Table 1: Parameters of the 150 MeV FFAG

Parameter	Value	
r_0	4.54	m
Cell structure	DFD	
N_{cells}	12	
k, field index	7.6	
Injection Energy	11	MeV
Extraction Energy	100 or 150	MeV
f_{rf}	1.6-5.2	MHz
B_{max}	1.6	T

CHARACTERISATION EXPERIMENTS

Two experimental periods in early to mid-2014 were allocated to characterisation of the FFAG. Here we describe a few selected results.

Injection Matching

The H⁻ beam follows a complex trajectory from the outside of the main ring magnets, through the open magnet side and in to the stripping foil. A simulation of this trajectory based on 3D design field maps, benchmarked in ZGOUBI [5] and an in-house code at KURRI, is shown in Fig. 2. Matching of position and angle at the stripping foil is achieved by adjusting horizontal and vertical steerers upstream. The vertical orbit is considered matched when the amplitude of coherent oscillations observed on the bunch monitors is minimised. For the purposes of characterisation experiments, horizontal orbit matching is adjusted empirically to maximise the number of circulating turns of a coasting beam at injection energy. In user operation this is optimised to give the best extracted beam current.
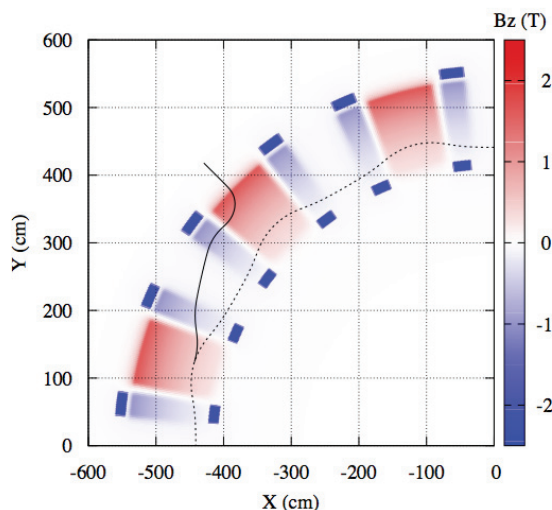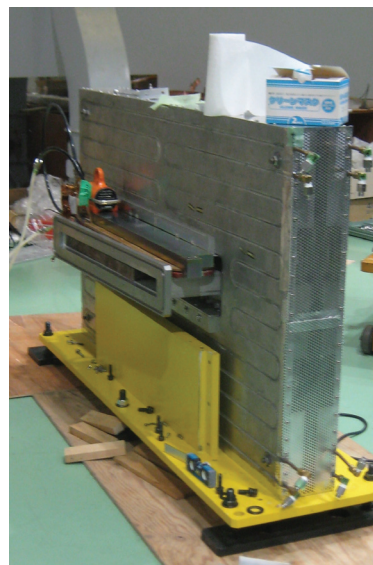

Figure 3: The broadband magnetic alloy rf cavity.

The rf cavity is located in one of the straight sections and is thought to be absorbing this stray field, breaking the symmetry of the ring and affecting the orbits and overall dynamics of the FFAG.

In late 2013 the rf cavity was temporarily removed to install new corrector magnets. With the cavity physically removed the opportunity was taken to test the assertion that the cavity is the main source of COD. A beam was injected into the ring and the closed orbit measured using three radial probes at different azimuthal locations around the ring. Despite being located at different azimuths, the probes are all in the centre of F magnets. As such the radial position of the orbit should be the same at all three locations. This was confirmed and no discernible COD was measured.

After re-installing the cavity the COD was re-measured, confirming that the major source of COD is the cavity itself. The new corrector poles were then tested to check how well they corrected the COD. Radial probes at three azimuthal locations were inserted into the ring and the time to loss of the beam was measured as a function of radius during acceleration. If there was no COD present, the three probes would measure the same time to loss at a given radius, as they are all located in the centre of F magnets. Thus for each corrector setting and for a given time, the deviation from the mean of the beam radius between the three probes gives us an estimate of the COD. The mean of the three probes is used as the zero point as there is no easily definable 'closed orbit' in an FFAG accelerator as there would be in a synchrotron.

The COD is fairly constant throughout the acceleration cycle, so can be represented simply as the average over time with a standard deviation error bar to indicating the variation of COD during the acceleration cycle. This is plotted for each probe in Fig. 4.

These results indicate that the corrector is reducing the COD, but further correction is still needed. Unfortunately the corrector excitation current was limited during this ex-

Figure 2: Injection trajectory of H⁻ beam shown as a solid line overlaid on the design B_z field. The dashed line corresponds to the circulating closed orbit and the stripping foil is located where the two paths intersect.

Closed Orbit Distortion

One of the most challenging aspects of this FFAG is the existence of a large closed orbit distortion (COD), consistent with a single large perturbation at the location of the rf cavity. The rf cavity shown in Fig. 3 is a broadband cavity employing magnetic alloy material [6] which was thought to be absorbing stray magnetic field from the main magnets and thus affecting the closed orbit.

The drawback of the yoke-free magnet design is that the magnets have been found to produce significant stray field.

perimental run to a maximum of 700 A. Correction of the COD is a priority and work is continuing on this, including changing the corrector power supply to increase the field provided.
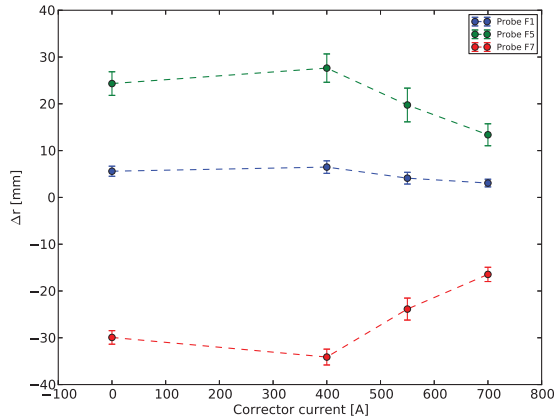

Figure 4: Closed orbit distortion quantified in terms of the variation in radial beam position from the mean at three different azimuthal locations, averaged over the acceleration cycle.

Dispersion in the Main Ring

The dispersion was measured in the injection line, at the position of the stripping foil and in the main ring. Figure 6 shows the dispersion in the main ring measured using the same three radial probes as in the closed orbit distortion measurement. The dispersion can be calculated using the radius vs time radial probe data where momentum values are inferred from the applied rf programme shown in Fig. 5.

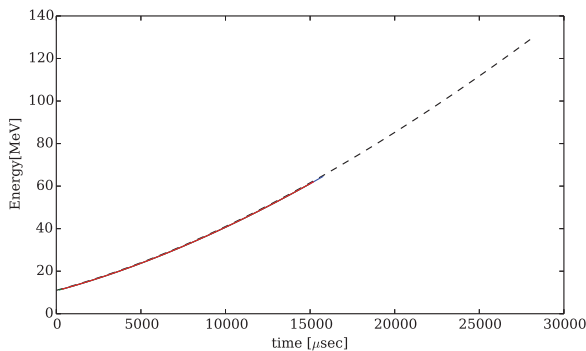$$D = \frac{\Delta r}{dp/p} \qquad (2)$$

Figure 5: Energy gain vs time of the applied rf pattern. The red line corresponds to the part used for analysis of the dispersion data.

Ideally all three results would be identical, but the discrepancy between them arises due to the presence of closed orbit
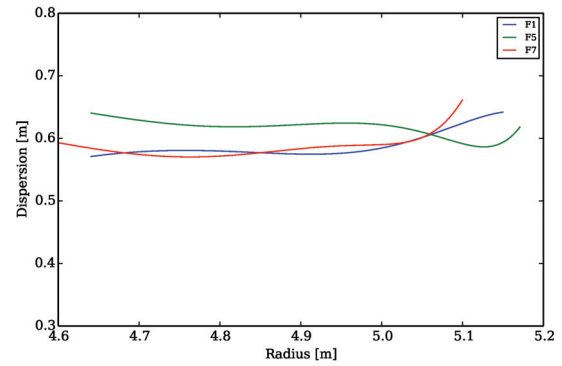

Figure 6: Dispersion in the ring as a function of radius measured using three different radial probes.

distortion. This is currently being studied in detailed simulations. However, the measurement shows that the dispersion is close to the design value of D=0.55 m at the centre of the F magnet.

Field Index

The field index, k, is defined in the design procedure to be 7.6, but in reality the field produced by the magnets does not follow the scaling law of Eq. 1 perfectly. We can define an effective field index which can then be measured throughout the acceleration cycle based on the revolution frequency and radial beam position variation.

$$k = \gamma^2 \frac{df/f}{dr/r} - (1 - \gamma^2) \qquad (3)$$

The frequency is obtained from the rf programme and the radial beam position is measured throughout the acceleration cycle. The relativistic γ factor is inferred from the rf programme. The measured effective field index is shown in Fig. 7, where again there is a discrepancy between the three measurements of the different radial probes.
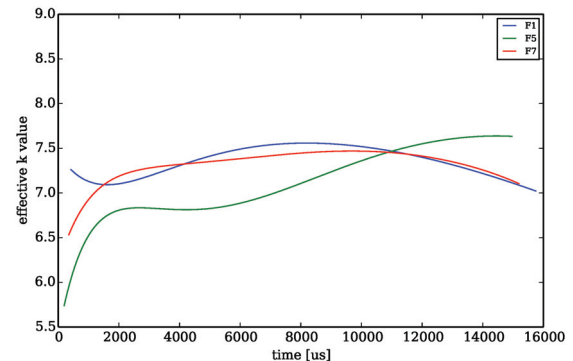

Figure 7: Effective field index, k, as a function of time during the acceleration cycle measured using three different radial probes.

Betatron Tunes

A number of methods can be used to measure the betatron tunes in this machine. The results shown in Fig. 8 were obtained using horizontal and vertical rf 'perturbator' devices and analysing the bunch turn-by-turn data using a real time spectrum analyser to find sidebands in the frequency spectrum. This required the design and implementation of a range of devices including a radially movable horizontal rf perturbator device and radially movable horizontal triangle BPM.
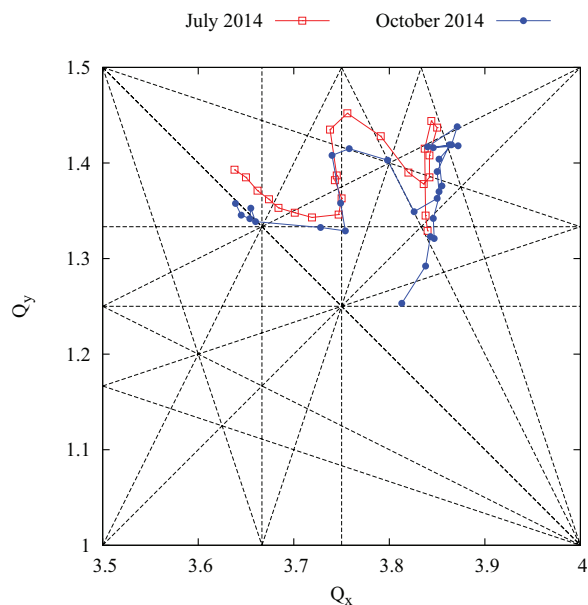

Figure 8: Measured horizontal and vertical ring tunes (Q_x, Q_y) throughout acceleration measured in July 2014 and an additional recent measurement in October 2014 with adjusted F/D ratio and after removal of unnecessary magnetic material.

Effects of the Stripping Foil

A key issue in this FFAG for high intensity operation is the effect of the stripping foil on the beam. In order to perform detailed studies at high intensity it is desirable to be able to measure the increase in beam emittance caused by space charge effects. This will compete with the emittance growth from foil scattering as the beam passes many times through the stripping foil at injection.

It is also necessary to understand the energy loss of the beam as it passes through the foil. Simulation work has been performed to study the energy loss and energy distribution after passing through the foil multiple times. An experimental measurement of the energy loss per turn in the foil has been carried out to measure the synchronous phase as a function of rf voltage. Analysis of the experimental data is in progress.

DISCUSSION AND FUTURE PLANS

Although the present beam intensity is sufficient for ADS experiments, there remains substantial beam loss throughout the acceleration cycle, as shown in Fig. 9. The major loss point is right after injection, with other loss points corresponding to resonance lines in the tune diagram.
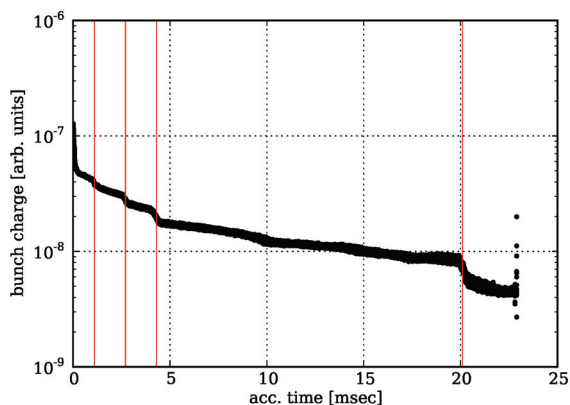

Figure 9: Present beam loss throughout the acceleration cycle. Major loss points marked with red lines occur at 1.1 ms, 2.7 ms, 4.3 ms and 20.1 ms.

A multi-faceted approach will enable the machine to operate with a higher average beam power.

It is clear that the dominant loss point is at the point of injection, where only roughly 10 to 40% of the beam survives depending on choice of phase and quality of injection matching. Optimisation of the rf pattern should improve this in future, but only to a limited extent.

One suspected additional source of imperfection in the ring was the presence of additional iron-based magnets from the previous injector. This additional iron was recently removed and the working point adjusted slightly, however no improvement was discernible in terms of beam loss. This is because the adjusted working point lies close to a betatron resonance, as can be clearly seen in the tune diagram. Further adjustment of the working point should improve this.

The installation of a second rf cavity is planned in early 2015 in order to increase the repetition rate from 20 Hz to 100 Hz. Faster acceleration should pull the beam off the foil more quickly and also reduce the impact of losses due to resonance crossing effects.

To reduce beam loss further the matching at injection needs to be optimised to reduce multiple scattering on the foil and reduce emittance growth. This is a key item to be measured and the use of a wire scanner is being investigated. Multiple scattering will also be reduced by an increase in the acceleration rate so the beam moves off the foil more quickly at injection.

The other key to enabling high power operation is an accurate model of the machine. A lot of work has been carried out at KURRI toward modelling this machine previously. To enhance these studies a detailed simulation campaign

is underway including code benchmarking, comparison to experiment and a parallel strand of code development and wider investigation into high intensity effects in FFAG accelerators.

REFERENCES

[1] M. Tanigaki, K. Mishima, and S. Shiroya, "Construction of FFAG accelerators in KURRI for ADS study", EPAC'04, Lucerne, July 2004, pp. 2676, `http://www.JACoW.org`.

[2] C. H. Pyeon et al., J. Nucl. Sci. Technol., vol. 46, no. 12 (2009) pp. 1091.

[3] T. Adachi et al., "A 150 MeV FFAG synchrotron with 'Return-Yoke Free' magnet", PAC 2001, Chicago, pp. 3254,

[3] T. Adachi et al., "A 150 MeV FFAG synchrotron with 'Return-Yoke Free' magnet", PAC 2001, Chicago, pp. 3254, `http://www.JACoW.org`.

[4] K. Okabe et al., "Development of H- injection of proton-FFAG at KURRI", IPAC 2010, Kyoto, THPEB009, pp. 3897, `http://www.JACoW.org`.

[5] F. Méot, "The ray-tracing code Zgoubi - status," Nucl. Instruments Methods Phys. Res. Sect. A, 767 (2014) pp. 112.

[6] Y. Yonemura, et al. "Development of RF acceleration system for 150MeV FFAG accelerator". Nucl. Instruments Methods Phys. Res. Sect. A, 576.2 (2007), pp. 294.

[7] Y. Ishi et al., "Present status and future of FFAGs at KURRI and the first ADSR experiment", IPAC 2010, Kyoto, TUOCRA03, pp. 1327, `http://www.JACoW.org`.